Rayleigh noise mitigation in DWDM LR-PONs using carrier suppressed subcarrier-amplitude modulated phase shift keying

C. W. Chow[#], G. Talli, A. D. Ellis, and P. D. Townsend*

Photonic Systems Group, Tyndall National Institute and Department of Physics, University College Cork, Ireland
[#]Present address: Department of Photonics, National Chiao Tung University, 1001 Ta-Hsueh Road, Hsinchu, Taiwan
paul.townsend@tyndall.ie

Abstract: We demonstrate a novel Rayleigh interferometric noise mitigation scheme for applications in carrier-distributed dense wavelength division multiplexed (DWDM) passive optical networks at 10 Gbit/s using carrier suppressed subcarrier-amplitude modulated phase shift keying modulation. The required optical signal to Rayleigh noise ratio is reduced by 12 dB, while achieving excellent tolerance to dispersion, subcarrier frequency and drive amplitude variations.

OCIS codes: (060.2330) Fiber optics communications; (060.4510) Optical communications.

References and links

1. R. Davey, J. Kani, F. Bourgart, and K. McCammon, "Options for future optical access networks," IEEE Commun. Mag. **44**, 50-56 (2006).
2. D. P. Shea, A. D. Ellis, D. B. Payne, R. P. Davey, and J. E. Mitchell "10 Gbit/s PON with 100 km reach and x1024 split," Proc. of ECOC, Rimini, Italy, 2003, Paper We.P.147.
3. G. Talli, C. W. Chow, P. D. Townsend, R. Davey, T. D. Ridder, X. -Z. Qiu, P. Ossieur, H. -G. Krimmel, D. Smith, I. Lealman, A. Poustie, S. Randel, H. Rohde, "Integrated metro and access network: PIEMAN," Proc. of NOC, Sweden, 2007.
4. R. D. Feldman, "Crosstalk and loss in wavelength division multiplexed systems employing spectral slicing," J. Lightwave. Technol. **15**, 1823–1831 (1997).
5. P. Healey, P. Townsend, C. Ford, L. Johnston, P. Townley, I. Lealman, L. Rivers, S. Perrin, and R. Moore, "Spectral slicing WDM-PON using wavelength-seeded reflective SOAs," Electron. Lett. **37**, 1181–1182 (2001).
6. S. -J. Park, C. -H. Lee, K. -T. Jeong, H. -J. Park, J. -G. Ahn, and K. -H. Song, "Fiber-to-the-home services based on wavelength-division multiplexing passive optical network," J. Lightwave. Technol. **22**, 2582–2591 (2004).
7. L. Y. Chan, C. K. Chan, D. T. K. Tong, F. Tong, and L. K. Chen, "Upstream traffic transmitter using injection-locked Fabry–Pérot laser diode as modulator for WDM access networks," Electron. Lett. **38**, 43–45 (2002).
8. Z. Li, Y. Dong, Y. Wang, and C. Lu, "A novel PSK-Manchester modulation format in 10-Gb/s passive optical network system with high tolerance to beat interference noise," IEEE Photon. Technol. Lett. **17**, 1118–1120 (2005).
9. T. Yoshida, S. Kimura, H. Kimura, K. Kumozaki, and T. Imai, "A new single-fiber 10-Gb/s optical loopback method using phase modulation for WDM optical access networks," J. Lightwave Technol. **24**, 786-796 (2006).
10. C. W. Chow, G. Talli, and P. D. Townsend, "Rayleigh noise reduction in 10-Gb/s DWDM-PONs by wavelength detuning and phase-modulation-induced spectral broadening," IEEE Photon. Technol. Lett. **19**, 423-425 (2007).
11. G. Talli, C. W. Chow, E. K. MacHale, and P. D. Townsend, "Long reach hybrid DWDM-TDM PON with high split ratio employing centralized light source," J. Opt. Netw. **6**, 765-776 (2007).
12. O. Leclerc, P. Brindel, D. Rouvillain, E. Pincemin, B. Dany, E. Desurvire, C. Duchet, E. Boucherez, S. Bouchoule, "40 Gbit/s polarization-insensitive and wavelength-independent InP Mach-Zehnder modulator for all-optical regeneration," Electron. Lett. **35**, 730-732 (1999).
13. G. Talli, D. Cotter, and P. D. Townsend, "Rayleigh backscattering impairments in access networks with centralised light source," Electron. Lett. **42**, 877-879 (2006).

#87487 - $15.00 USD Received 19 Oct 2007; revised 18 Dec 2007; accepted 26 Dec 2007; published 28 Jan 2008

1. Introduction

Demand for new high bandwidth services as well as changing competitive and regulatory forces are beginning to drive the deployment of fiber access networks around the world. One of the most attractive optical access architectures is the passive optical network (PON), which is highly cost-effective because the infrastructure is shared by many customers and has no active components, such as electronic switches, between the head-end office and the customer. The first generations of Gigabit PONs [1] typically offer 1 to 2.5 Gbit/s downstream and ~1 Gbit/s upstream, shared between 32 customers via passive optical splitters and a time-division multiple access protocol, over a reach of up to 20 km. Whilst these PONs offer significant bandwidth increases compared to copper-based approaches, they may not provide the best ultimate solution for service providers seeking to significantly reduce the cost of delivering future broadband services to customers in order to sustain profit margins. Hence research attention has recently turned to more radical network solutions based on new types of optically amplified, large split (~1000), long reach (~100km) PONs (LR-PONs), which are designed to allow individual customers to directly access bandwidths of up to 10 Gbit/s upstream and downstream [2]. These LR-PONs would replace the separate metro and access portions of the current network with a single integrated system. This approach is predicted to generate significant capital and operational cost savings for network operators, since the number of network elements and interconnection interfaces is reduced, along with the design complexity, footprint and electrical power consumption of the network as a whole.

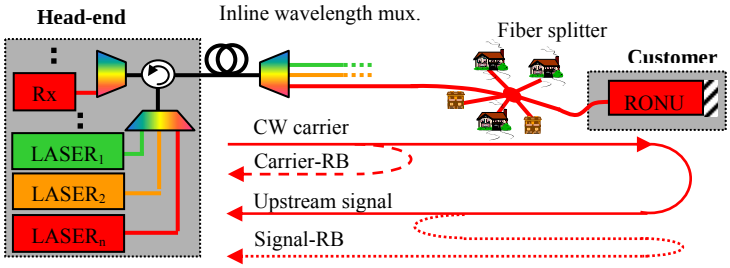

Fig. 1. Schematic of the RB contributions in a carrier-distributed DWDM-PON.

DWDM can also be employed in LR-PONs to enable a number of such networks, each working at different wavelengths, to share the same amplifiers and backhaul fiber across the metro part of the network [3]. One great challenge in these DWDM LR-PONs is the transmitter at the optical networking unit (ONU), located in the customer premises, which must have a wavelength that is precisely aligned with a specifically allocated DWDM grid wavelength. A cost-effective solution would ideally employ the same components in each ONU, which should thus be independent of the wavelength assigned by the network – or "colorless". Various solutions have been proposed for the colorless ONUs [4-7]. However, these approaches are limited by various combinations of limited modulation bandwidth [4, 5] and high chirp [6, 7], both of which significantly restrict the overall capacity and reach of the PON. For these reasons, ONU designs based on conventional modulators, such as Mach-Zehnder modulators (MZM) or semiconductor electroabsorption modulators, are more favorable for applications in 10 Gbit/s DWDM LR-PONs. As illustrated in Fig. 1, in this approach each ONU operates in reflective mode (RONU) generating upstream signals from a continuous wave (CW) carrier distributed from the head-end office. The downstream signals, which are not shown in Fig. 1, are carried by a separate wavelength.

Although the carrier-distributed DWDM LR-PONs have many attractive features, a key issue that needs to be addressed is how best to control the impairments that can arise from optical beat noise induced by back-reflections and Rayleigh backscattering (RB) of the optical carrier at the upstream receiver (Rx) at the head-end office. Advanced modulation formats [8-

#87487 - $15.00 USD Received 19 Oct 2007; revised 18 Dec 2007; accepted 26 Dec 2007; published 28 Jan 2008

10] can be used to mitigate the impact of RB in carrier-distributed PONs. A previously reported RB mitigation scheme using phase modulation (PM) to spectrally-reshape the upstream signal, called phase-modulated non-return-to-zero (PM-NRZ), is effective against RB induced interference, but requires two optical modulators and, furthermore, highly degrades the chromatic dispersion tolerance of the signal due to the generation of multiple Bessel sidebands [10]. Here we propose and quantitatively analyze a significantly improved scheme, namely carrier suppressed subcarrier amplitude modulated phase shift keying (CSS-AMPSK), which is shown to be highly effective at mitigating noise generated by RB. In addition to improving the RB tolerance of the system, this scheme has excellent tolerance to dispersion, subcarrier-frequency and drive-amplitude variations.

2. Rayleigh noise and impact of modulation format

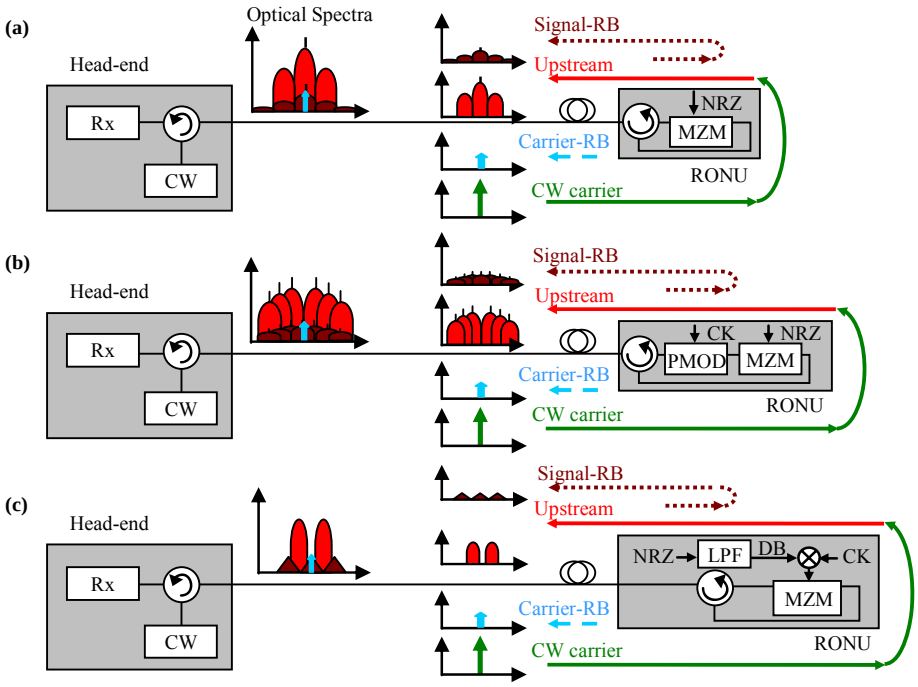

Fig. 2. Schematic of MOD configurations and optical spectra of (a) NRZ, (b) PM-NRZ and (c) CSS-AMPSK. The wavelength multiplexers are not shown for clarity. MZM: Mach-Zehnder modulator, PMOD: phase modulator, CK: sinusoidal clock signal, LPF: low pass filter.

Figure 1 shows the two dominant contributions to the RB in carrier-distributed PONs, which interfere with the upstream signal at the Rx. The first contribution, Carrier-RB, is generated by the backscatter of the CW carrier being delivered to the RONU. The second contribution, Signal-RB, is generated by the modulated upstream signal at the output of the RONU. Backscattered light from the upstream signal re-enters the RONU, where it is re-modulated and reflected towards the Rx. The Carrier-RB has the same spectrum as the CW carrier, while the Signal-RB is modulated twice by the RONU and has a broader spectrum. The relative impact of the two components depends on the exact network configuration and hence, for a full understanding, separate analysis of each effect is carried out.

Figure 2 shows schematics of various reflective modulator configurations for carrier-distributed PONs including conventional NRZ, PM-NRZ [10] and the proposed CSS-AMPSK modulation formats, with the corresponding schematic optical spectra: in green CW carrier; red upstream; blue Carrier-RB; and brown Signal-RB. For efficient Raleigh noise mitigation

#87487 - $15.00 USD Received 19 Oct 2007; revised 18 Dec 2007; accepted 26 Dec 2007; published 28 Jan 2008

it is important to minimize the spectral overlap between the upstream signal and both types of RB, ensuring that the majority of the frequency components of the resultant electrical beat noise fall outside the 10 Gbit/s Rx bandwidth (typically 7.5 GHz). In Fig. 2(a), the vulnerability of NRZ modulation to both Signal-RB and Carrier-RB is revealed by the strong overlap of all three spectra. If we employ the PM-NRZ scheme of Fig. 2(b), the generation of multiple Bessel sidebands and suppression of the center wavelength reduce the overlap with the unmodulated Carrier-RB, but is less effective against the double modulated Signal-RB. In Fig. 2(c), CSS-AMPSK is generated by driving a Mach-Zehnder modulator (MZM) with an AMPSK drive signal, itself generated by modulating a 10 GHz sine clock signal with a 10 Gbit/s duobinary (DB) signal using a microwave mixer. In practice the DB signal is generated from the NRZ signal using a low pass filter (LPF). By biasing the MZM for minimum transmission the CW carrier wavelength is suppressed, and two copies of the AMPSK drive signal are translated to sub-carriers at ±10 GHz with respect to the optical carrier frequency. The fundamental frequency shift associated with subcarrier drive of a MZM biased for minimum transmission ensures a frequency translation each time a signal passes through the modulator, ensuring that the upstream signal is shifted away from the backscattered CW signal, and the Signal-RB components are further shifted away from the upstream signal. Hence, the CSS-AMPSK is expected to have strong tolerance to both RB components, as explained in more in detail in Section 4.

3. Experiment

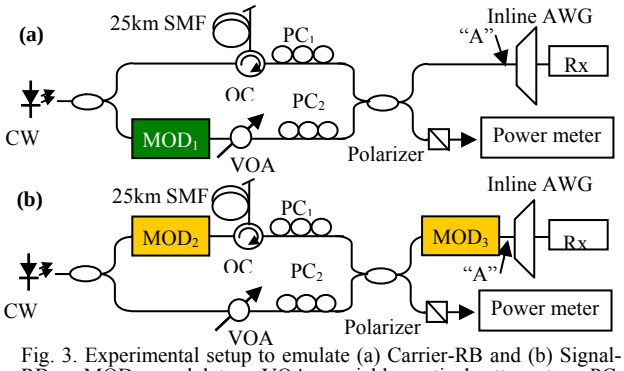

Fig. 3. Experimental setup to emulate (a) Carrier-RB and (b) Signal-RB. MOD: modulator, VOA: variable optical attenuator, PC: polarization controller, AWG: array waveguide grating.

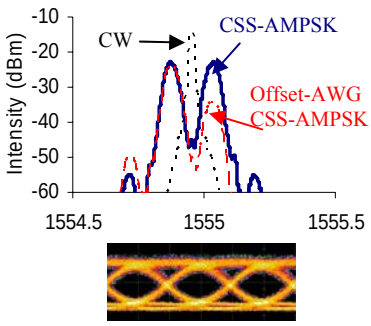

Fig. 4. Optical spectra and back-to-back eye diagram of CSS-AMPSK.

Figure 3 (a) and (b) show the experimental setups used to analyze the Raleigh noise tolerance of the CSS-AMPSK upstream signal, which simulates the impairments of a real PON by generating two interfering signals in different arms of an interferometer. The modulator configurations (MODs) are as shown in Fig. 2(c), but now operating in transmission mode without the optical circulator. By locating the modulators at different points in the setup it is possible to emulate the Carrier- and Signal- Rayleigh components that would be expected in a real carrier-distributed network employing RONUs [10]. For Carrier-RB analysis [Fig. 3(a)], MOD_1 is used to generate the data signal and the Carrier-RB is generated by the unmodulated carrier propagating through 25 km of standard single mode fibre (SMF). On the other hand, for Signal-RB analysis [Fig. 3(b)], the remodulated backscattering is generated by firstly modulating the optical signal with MOD_2. The remodulation of the backscattered signal generated by the 25km SMF is then emulated by MOD_3. At the receiver, this interferes with the emulated upstream signal, generated by a CW carrier delivered via the lower arm and simultaneously modulated by MOD_3. In both experiments a variable optical attenuator (VOA) is used to vary the signal power and so generate different optical signal to Rayleigh noise ratios (OSRNRs). The latter is defined as the ratio of total signal and total RB power at the

#87487 - $15.00 USD Received 19 Oct 2007; revised 18 Dec 2007; accepted 26 Dec 2007; published 28 Jan 2008

input to the inline arrayed waveguide grating (AWG) (point "A" in Fig. 3). All signals are directly detected without further demodulation in an optically pre-amplified Rx, which also contains an identical 100 GHz Gaussian AWG with 3dB-width of 50 GHz. Both AWGs are offset by ~30GHz to filter selectively one of the sub-carriers of the CSS-AMPSK signal, which increases the RB noise mitigation and reduces subcarrier fading [11].

The CSS-AMPSK modulator configuration [Fig. 2(c)] consists of a double balanced mixer with an electrical 10 GHz clock (CK) connected to the local oscillator (LO) input. In practice, the clock may be recovered from the downstream signal, which operates in continuous mode. The 10 Gbit/s PRBS 2^{31}-1 NRZ baseband data is effectively duobinary filtered by an electrical LPF with passband DC-3.2GHz at the intermediate frequency (IF) input of the mixer. The mixer performs a radio frequency (RF) up-conversion of the duobinary data and is biased for minimum transmission at the mid level of the duobinary eye. At the mixer RF output, an electrical 10 Gbit/s AMPSK signal on a 10 GHz carrier is generated, where the outer rails of the duobinary signal produce equal amplitude outputs of opposite phase, and the middle level produce a low amplitude output of alternating phase. There is no particular synchronization requirement between the electrical sine wave and baseband data. The mixed signal, with a peak-to-peak voltage V_{pp} ~0.9 V_{π}, drives MZMs at each MOD location, each biased at its transmission minimum generating two AMPSK modulated subcarriers at ±10 GHz, as shown by the experimental optical spectra in Fig. 4. The proof of concept experiments used commercially available $LiNbO_3$ MZMs, but alterative schemes using polarization insensitive semiconductor modulators could be more practical [12].

4. Results and discussion

Figure 4 shows the experimental optical spectra of the CW carrier, the CSS-AMPSK modulated signal and the same signal after filtering using the offset-AWG. The 3 dB bandwidth of each subcarrier of the CSS-AMPSK spectrum is about 5.5 GHz, as found for a conventional AMPSK (also known as optical duobinary) signal. The detected eye diagram of CSS-AMPSK, as shown in Fig. 4 is similar to that for conventional NRZ modulation, and shows the characteristic zero level ripples associated with AMPSK formatted data.

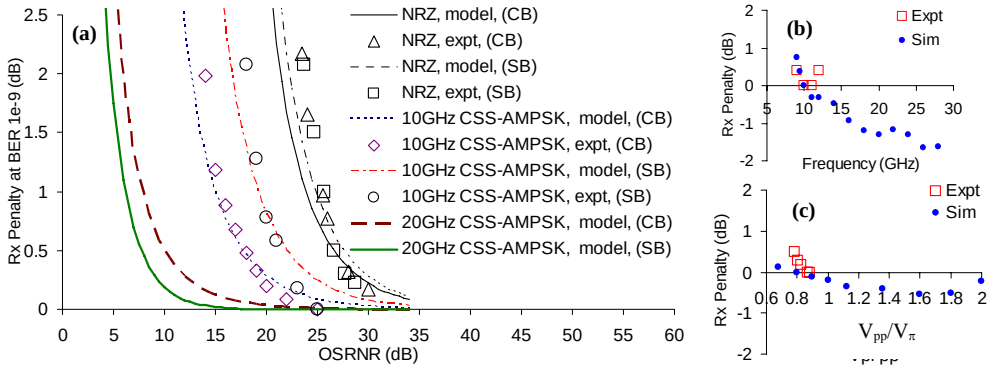

Fig. 5. (a) RB noise performance at different OSRNR of CSS-AMPSK when compared with conventional NRZ formats. Tolerance of CSS-AMPSK to variations of (b) subcarrier frequency and (c) drive amplitude.

Figure 5(a) shows the experimental and modeled power penalties at a bit error rate (BER) of 10^{-9} for the blue-side CSS-AMPSK (selected by the offset-AWG) and NRZ signals (for comparison) at 10 Gbit/s as a function of OSRNRs. For NRZ, even relatively low levels of RB can significantly degrade the BER due to the complete spectral overlap between upstream signal and RB components. The CSS-AMPSK improves the required OSRNR (at 1 dB penalty) by 12 and 7 dB in the Carrier-RB and Signal-RB cases respectively. In a RB noise-limited PON this enables split ratios to be increased by 4× or 16× in typical single and dual

#87487 - $15.00 USD Received 19 Oct 2007; revised 18 Dec 2007; accepted 26 Dec 2007; published 28 Jan 2008

feeder fiber configurations, respectively [11]. Results from the model (using the approach developed in [13]) are in good agreement with the experiments. The mitigation of the Carrier-RB is obtained due to a combination of two separate effects. Firstly, the compact spectrum of CSS-AMPSK has less spectral overlap with the CW carrier, reducing the total beat noise power in the Rx. Secondly, the optical power of the Carrier-RB is concentrated at the CW carrier frequency, which is more strongly attenuated by the offset-AWG than the blue-side CSS-AMPSK signal, whose power is concentrated at +10 GHz. For Signal-RB, when the backscattered CSS-AMPSK is re-modulated in the RONU, the additional frequency shifts will transform odd harmonic components of the drive signal (±10 GHz) to even harmonics (0 and ±20 GHz). The spectral overlap of the upstream signal and the Signal-RB is small due to the compact spectrum of the AMPSK modulation, but bigger than the Carrier-RB case. The optical filtering is also less effective since the +20 GHz component is within the AWG bandwidth. Hence experimental and modeling results show a slightly worse performance in the Signal-RB case. However, modeling results also show that >17 dB overall OSRNR improvement is possible if a RF frequency doubler is used to increase the subcarrier frequency to 20 GHz, which further reduces the spectral overlap in both the Carrier- and Signal-RB cases and also improves the effectiveness of the offset-AWG filtering.

The CSS-AMPSK also offers several practical advantages for use in cost sensitive RONUs. Firstly, there are no synchronization requirements between the electrical subcarrier and the electrical data. The experimental and numerical analysis (using VPI Transmission Maker V6.5) in Fig. 5(b) show that provided the subcarrier-frequency is sufficient to ensure that spectral overlap of the red- and blue-sidebands of the CSS-AMPSK signal is small, excellent back-to-back performance is obtained. Experimentally, <1 dB penalty was observed when the LO frequency was tuned between 9-12 GHz. The disagreement between modeling and experiments for high frequency is only due to the limited bandwidth of the RF mixer. Secondly, due to the subcarrier modulation format, the modulation unit is resilient to the drive-amplitude, as shown in Fig. 5(c). Good performance is observed from drive amplitudes from V_{pp}=0.7 V_{π}, where the optical carrier is sufficiently suppressed to mitigate Carrier-RB, up to V_{pp}=2 V_{π}, when the third-order harmonics (at ±30 GHz) start to become more dominant. Experimentally, <1 dB penalty was observed when the drive amplitude, V_{pp}, was varied between 0.8 and 0.9 V_{π} (limited by the maximum output voltage of the RF amplifier).

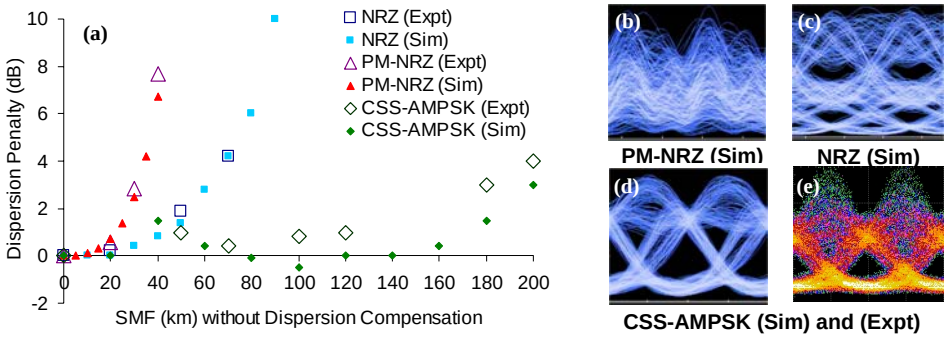

Fig. 6. (a) Dispersion penalties of PM-NRZ, NRZ and CSS-AMPSK signals without dispersion compensation. 10 Gb/s eye diagrams of simulated (b) PM-NRZ, (c) NRZ, (d) CSS-AMPSK and (e) experimental CSS-AMPSK signals at 200km transmission without dispersion compensation.

Dispersion tolerance is important for PON applications, since they are normally not dispersion compensated for reasons of cost and practicality (the fiber lengths between the head-end office and each ONU will vary). This is particularly so when bit rate and reach is increased as in a 10 Gbit/s LR-PON. Figure 6(a) compares the dispersion tolerance of 10 Gbit/s NRZ, PM-NRZ and CSS-AMPSK signals with the corresponding eye diagrams after 200 km of SMF transmission without dispersion compensation. The results show that, whilst

#87487 - $15.00 USD Received 19 Oct 2007; revised 18 Dec 2007; accepted 26 Dec 2007; published 28 Jan 2008

the PM-NRZ and NRZ eyes close completely [Fig. 6(b), (c)], a clear open eye of CSS-AMPSK can be observed [Fig. 6(d)]. There is a good match in eye-shape of the CSS-AMPSK between simulation [Fig. 6(d)] and experiment [Fig. 6(e)]. CSS-AMPSK offers strong dispersion tolerance with <1 dB power penalty without dispersion compensation for ranges beyond 100 km, making it potentially suitable for use in DWDM LR-PONs.

5. Conclusion

We have proposed and demonstrated a novel Rayleigh-noise mitigation scheme for 10 Gbit/s carrier-distributed DWDM LR-PONs using CSS-AMPSK modulation. The observed tolerance to Carrier-RB and Signal-RB compares favorably to those of the conventional NRZ and the prior-art PM-NRZ formats. Experimental and simulation results suggest that CSS-AMPSK may be an excellent candidate for high split LR-PONs, combining a single modulator and minimum control in RONU, with good tolerance to RB and dispersion.

Acknowledgements

We acknowledge Science Foundation Ireland support under grant: 03/IN1/1340 and 06/IN/I969 and Dr. A. Kaszubowska for useful discussions.

#87487 - $15.00 USD Received 19 Oct 2007; revised 18 Dec 2007; accepted 26 Dec 2007; published 28 Jan 2008